Simulated power spectral density (PSD) of background electrocorticogram (ECoG)

Cognitive Neurodynamics 3(1): 97-103 (2009)

Walter J Freeman
Department of Molecular & Cell Biology
University of California at Berkeley, CA 94720-3206 USA
dfreeman@berkeley.edu

Jian Zhai
Department of Mathematics
Zhejiang University, Hangzhou 310027, China
jzhai@zju.edu.cn

Running head: Power-law exponents of electrocorticogram

Key words: cortex, background activity; black noise; electrocorticogram ECoG; power-law distribution; power spectral density PSD;

Abstract

The ECoG background activity of cerebral cortex in states of rest and slow wave sleep resembles broadband noise. The power spectral density (PSD) then may often conform to a power-law distribution: a straight line in coordinates of log power vs. log frequency. The exponent, x, of the distribution, $1/f^x$, ranges between 2 and 4. These findings are explained with a model of the neural source of the background activity in mutual excitation among pyramidal cells. The dendritic response of a population of interactive excitatory neurons to an impulse input is a rapid exponential rise and a slow exponential decay, which can be fitted with the sum of two exponential terms. When that function is convolved as the kernel with pulses from a Poisson process and summed, the resulting "brown" or "black noise conforms to the ECoG time series and the PSD in rest and sleep. The PSD slope is dependent on the rate of rise. The variation in the observed slope is attributed to variation in the level of the background activity that is homeostatically regulated by the refractory periods of the excitatory neurons. Departures in behavior from rest and sleep to action are accompanied by local peaks in the PSD, which manifest emergent nonrandom structure in the ECoG, and which prevent reliable estimation of the $1/f^x$ exponents in active states. We conclude that the resting ECoG truly is low-dimensional noise, and that the resting state is an optimal starting point for defining and measuring both artifactual and physiological structures emergent in the activated ECoG.

1. Introduction

The "spontaneous" background activity of cerebral cortex is essential for perception, cognition, and all other intentional behaviors. It places great demands on bodily metabolism even in brains at rest, consuming what is referred to as "dark energy" [Raichle, 2006]. Its role is comparable to that of temperature regulation in warm-blooded animals. Though the maintenance of constant high body temperature and brain readiness is very costly, it is indispensible for survival in a competitive world. Just as body

temperature is controlled by homeostasis in health and fever, the level of dark energy in the brain is regulated by feedback mechanisms having a variable set point in sleep and arousal. The properties of that mechanism are revealed by analysis of the background activity [Freeman, 2004a,b; 2005; 2006a; reviewed in Freeman, 2006b, 2007].

The background is observed in two forms of electrical activity. The axons of cortical neurons generate spikes that in resting cortex form aperiodic spike trains. Commonly the background trains have flat autocorrelations after a brief absolute refractory period (zero probability) followed by the relative refractory period (an approximately exponential rise in firing probability with or without an overshoot to the mean pre-firing level_. The randomness of the spike trains is shown by interval histograms that conform to the exponential distribution of a Poisson process modified by the refractory periods; the cross-correlations among spike trains that tend to be vanishingly small [Abeles, 1991]. The dendrites of neurons generate synaptic currents that in recordings from the surface of the resting cortex (the electrocorticogram, ECoG) give broad-spectrum oscillations. The temporal power spectral densities (PSD) in coordinates of log power vs. log frequency (Fig. 1) often conform to power-law distributions ($1/f^x$) with exponents x varying between 0 and 4 [slopes of 0 to -4 in rabbit (A-C) [Freeman, 2006a] and human (D) [Freeman et al., 2006]. The randomness in both pulse trains and ECoG usually gives way to less disordered activity as brains become engaged in intentional behavior.

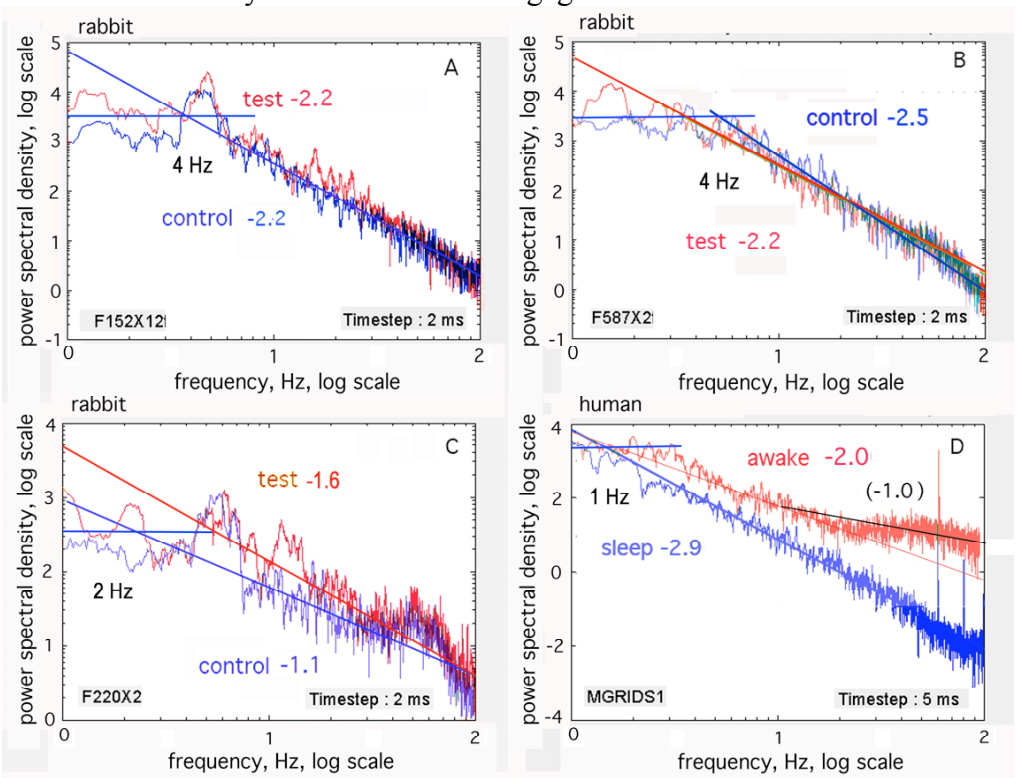

Fig. 1. Examples are shown of straight lines fitted to PSD (power/unit frequency in $\log_{10}$ scale) from ECoG in rabbit (**A-C**) and human (**D**) in contrasting states of relative behavioral inactivity vs. states of engagement. The lines were fitted by hand and eye in order to calculate the exponent, x, and to emphasize the appearance of peaks above the putative $1/f^x$ relation. The short line in (D) between 10-100 Hz was fitted by linear regression. Adapted from Freeman et al. [2006].

If the background activity really is noise, as first proposed by Elul [1972], then it should be possible to simulate the background activity by using a random number generator, in order to determine what kind of noise it is, and how it supports cognition. Recent studies of the background ECoG [Freeman, 2004a,b; 2005; 2006; reviewed in Freeman and Cao, 2008] provided evidence that the background activity is generated by mutual excitation among populations of cortical excitatory neurons, and that the level of the activity is stabilized everywhere locally by the refractory periods, not by inhibitory interneurons. The simplest model is provided by cumulative summation of detrended white noise [Freeman, 2006], which gives a $1/f^2$ power-law PSD after removal of the initiating transient. The limitation of this simple model is that the slope of the PSD is fixed at -2.
Moreover simply summing simulated action potentials cannot simulate the ECoG, because the ECoG is the output of the dendrites that are synaptically driven by the action potentials. The simulation by integration must be done by simulating the impulse response of cortex, which is done by fitting a curve to the cortical responses to single-shock electrical stimulation of an afferent pathway. This impulse response has the forms of a dendritic wave an averaged evoked potential (AEP) or a fluctuation in the firing density in a poststimulus time histogram (PSTH, Fig. 2). The impulse response shows a rapid rise and a prolonged return to the background level [Freeman, 1974, 1975], owing to the reverberation of firing among the thousands of neurons transmitting and re-transmitting to each other. The refractory periods are not seen directly; they are indirectly revealed by slowing of the rise rate and quickening of the decay rate, when the strength of the driving impulse input is increased, which forces more neurons to fire and then become refractory.

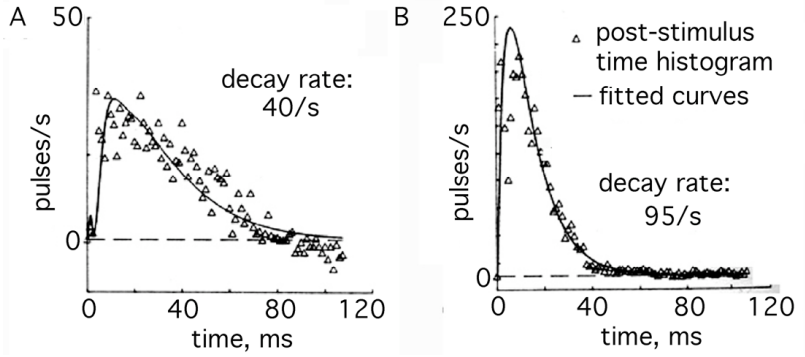

Fig. 2, A. Two examples of the impulse responses of the bulbar periglomerular mutually excitatory population at lowest and highest stimulus intensities give decay rates respectively of b = 40/s and 90/s and rise rates respectively of 500/sec and 300/sec. Adapted from Freeman [1974].

Conversely, when the driving input is reduced, the rise rate, β, increases and the decay rate, β, decreases and extrapolates to zero at threshold (Fig. 3, B). This result implies that the background activity is self-regulated at a stable set point, at which the steady state is maintained (unity gain in the cortical feedback loop). It turns out that the dynamic state of the cortex depends heavily on the level of the self-stabilized background activity with respect to the level of background excitatory input that drives the cortex above its internally determined set point. The lower is the level of background set by refractory

periods or the higher is the ongoing input, the stronger is the blocking action of the refractory periods, and so also the steeper is the slope of the PSD of the ECoG. The role of inhibitory neurons is to introduce narrow band oscillations that appear as local peaks in the PSD that rise above the 1/f power-law distribution (Fig. 1, A), and that may decrease the slope below -2 as measured by least mean squares deviation from a fitted straight line (C, D).

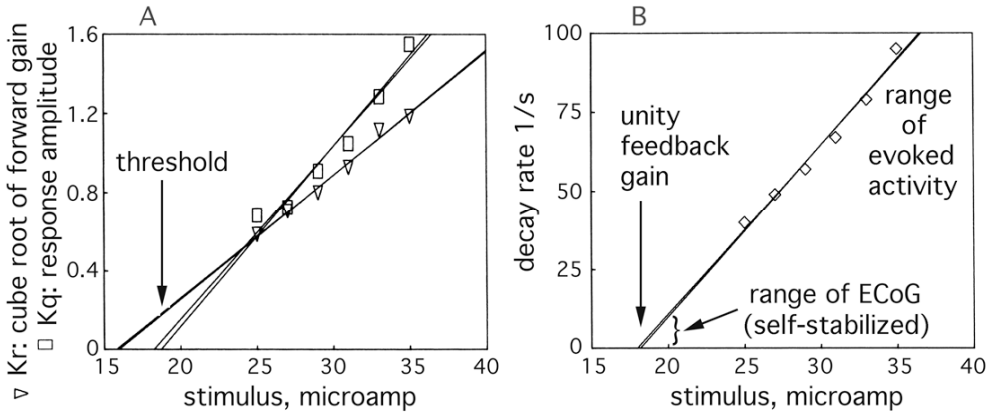

Fig. 3. A. Extrapolation of the relation of response amplitude as a function of stimulus intensity gives the threshold of the impulse response to an excitatory stimulus. B. Extrapolation of the measured rate constants to threshold gives the rate constant of zero at response amplitude of zero, which is evidence for the set point at which the background activity is stabilized by neurohumoral controls. That regulation is expressed in the limitations on neural firing rates imposed by their refractory periods. Adapted from Freeman [1974]

The aim of this report is focused on simulation of the variation in slope of the ECoG PSD by using random numbers [Freeman and Zhai, 2007], thereby to explain the role of the refractory periods of the spike activity, by which the level of the background activity is stabilized, in determining the slope of the PSD. The explanation is especially relevant to the change in slope of the PSD of human ECoG (Fig. 1, D), which averages near -2 in the awake state and near -3 in slow wave sleep [Freeman, et al., 2006].

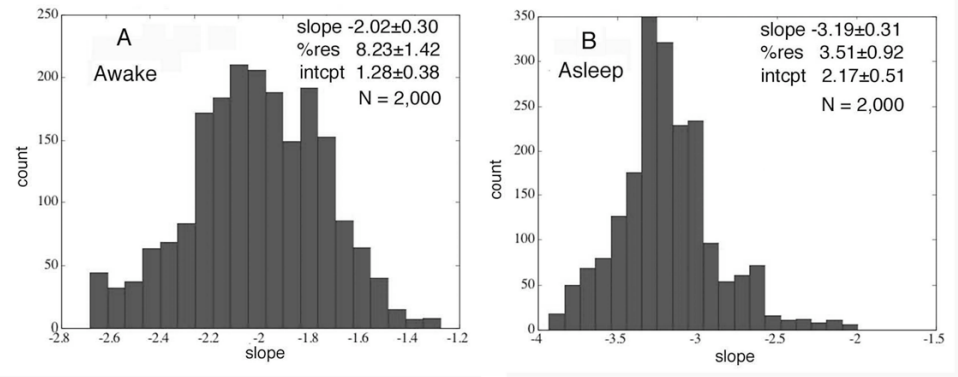

Fig. 4. Histograms of the slopes of PSD from human ECoG were constructed for the states of awake rest and slow wave sleep. A straight line was fitted b regression to each PSD in the frequency range from 3-100 Hz for calculation of the slope, the intercept, and the residuals expressed as % of the total variance in the designated frequency range. From Freeman et al. [2006].

2. Methods

The ECoG data used for simulation were drawn from three data banks. ECoG signals were recorded from an 8x8 array on a sensory cortex in 9 rabbits, each with 40 trials that consisted of 3 seconds pre-stimulus with no overt behavior and 3 seconds during a conditioned stimulus and response [Barrie, Freeman, and Lenhart, 1996]. Signals were digitized at 500 Hz with pass band 0.1-120 Hz. ECoG signals were recorded from the right inferior temporal gyrus of a neurosurgical patient implanted with an 8x8 epipial array for 8 days, with continuous recording during sleep, waking rest, task performance and seizure [Freeman et al., 2006a,b]. Records were filtered 0.1-100 Hz and down-sampled at 200 Hz. The third data set provided information about the impulse response of cortical excitatory neurons. This consisted of post-stimulus time histograms (PSTH) of single periglomerular neurons in the olfactory bulb responding to repeated single shock electric stimulation of the primary olfactory nerve over a range of stimulus intensities [Freeman, 1974]. Additionally interval histograms and autocorrelation functions were calculated from these and other neurons in the olfactory system and fitted with sums of exponential terms to derive the statistics of the background activity for simulation [Freeman, 1975].

For simulation of ECoG a time series in .001 ms steps was generated of spikes recurring at random intervals exponentially distributed with rate constant, γ, at the microscopic level in a nominal population of 1000 neurons firing independently at mean rates of γ = 0.1/s to γ = 10/s. There was a trade-off between nominal number of neurons and firing rate per neuron; all that was needed was sufficient pulse density to approximate the sum with a continuous function. The mean value, γ, merely scaled the power of the PSD without affecting the form, so low values were used for speed of computation. The population activity at the mesoscopic level was modeled by p(t) representing extracellular pulse density and v(t) representing extracellular wave density and the ECoG.

The response to single-shock electrical stimulation of an afferent pathway gave a compound postsynaptic potential with a rapid rise rate, β, and a slower decay rate, α, that could be approximately fitted with the sum of two exponential terms (Fig. 5, A):

$$v(t) \sim p(t) = k_e (\beta - \alpha) [\exp(-\alpha t) - \exp(-\beta t)], \qquad (1)$$

where k_e was the forward gain parameter and $(\beta - \alpha)$ normalized the output magnitude, p(t), with respect to the rate constants in fitting the increase in firing density of population activity above the mean background level after each spike occurrence, with corresponding increase in excitatory synaptic current associated with the increase in pulse density of neural output. The simulated evoked ECoG, v(t), was proportional to p(t) by an arbitrary conversion factor between wave density and pulse density [Freeman, 1975].

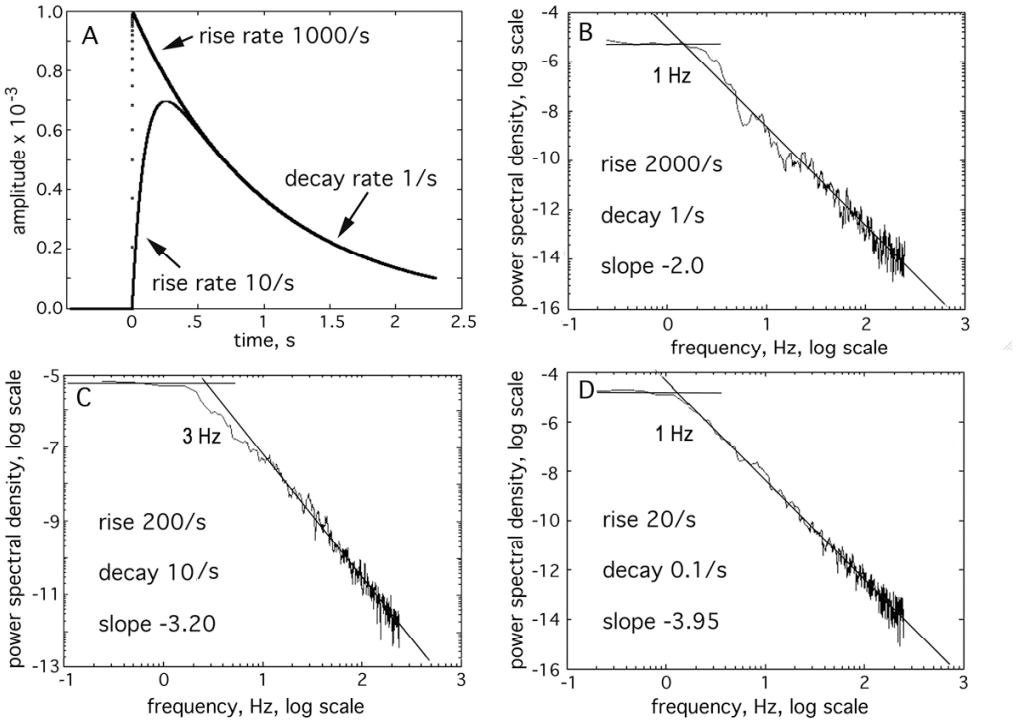

Fig. 5. A. Two examples are shown of the impulse response used as the kernel of integration for convolution with the Poisson process: α = 1/s, β = 1000/s or 10/s, step size 2 ms. **B-D.** Simulated PSD with the three filter settings illustrating the slopes and the roll-off frequencies.

Equation (1) specified a 2-stage linear low-pass filter. The PSD of its pass band for output with white noise input was flat for frequencies up to an inflection frequency determined by the decay rate, α (Fig. 5, B-D) Above that inflection the log power decreased linearly with increasing log frequency ($1/f^x$) with x bounded between 2 and 4. At the lower extreme of $\beta = 0$ and $\alpha = \infty$, equation (1) reduced to a single pole filter with the PSD slope = -2 (x = 2, "brown noise"). At the other extreme, the two rate constants were equal, $\beta = \alpha$, so that equation (1) was indeterminate. Textbooks in feedback control theory have shown in this case how equation (1) became $p(t) = \alpha\ t \exp(-\alpha\ t)$, with the PSD slope = -4 (x = 4. "black" noise [Schroeder, 1991]). The impulse response could then be approximated by the solution to a second order linear ordinary differential equation. Fitting equation (1) to the PSTH showed that, with increasing stimulus intensity and response amplitude, the value of α increased while β decreased [Freeman, 1975].

To simulate the mesoscopic spatiotemporal integration of the microscopic neural activity the Poisson spike train was convolved with the impulse response as the kernel of integration and down-sampled at 2 ms or 5 ms intervals corresponding to ECoG sampling times in research respectively in rabbit and human ECoG. Simulated data from the initial 2 s were omitted to insure that the cumulative sum reached a steady state. The duration of the kernel after each spike was terminated after $p(t) = 10^{-6}$. The PSD of the outputs of the

convolution in 10 s segments were estimated by a modified periodogram using the multitaper method [Percival and Walden, 1993] up to the Nyquist frequency (250 Hz or 100 Hz). The inflection frequency was set by α between 1 and 7 Hz by values of α = 100 ms, 1 s, and 10 s, and β was varied in steps of ¼ $\log_{10}$ from 3000/s to 10/s. Slopes of simulated ECoG were estimated by linear regression of a line fitted to the PSD between 10 and 100 Hz. Slopes of PSD from real ECoG were estimated by drawing a line through spectral segments delineating a $1/f^x$ baseline from which spectral peaks arose.

3. Results

3.1. Description of ECoG PSD in log-log coordinates

The slopes of PSD averaged near zero for low frequencies and were steep for high frequencies. The transitions at and near the roll-off frequencies (Fig, 1 and Fig. 4) were rounded and obscured by peaks. The simplest PSD were from a state of rest or sleep in human (D) and from the pre-stimulus control state of expectancy of a conditioned stimulus (A) prior to the test state containing the conditioned stimulus and response in rabbit [Freeman, 2005]. In data from 8 of the 9 rabbits the PSD of the control ECoG conformed to a power-law distribution (A), often with a theta peak. In the test period the power increased in multiple peaks, in some instances without significant change in slope (A) and in others with decreased slope and exponent x of the PSD. Data from 1 rabbit gave PSD with multiple peaks in both periods that increased in departure from rest (C). The power-law form was not apparent. Fitting a line to these complex PSD commonly gave slopes ranging between 0 and -2. Fig. 1, D "awake" illustrates the two techniques used to measure the slopes of PSD: by hand or by linear regression. Most subjects provided at least one PSD that conformed to $1/f^x$, in which case the two estimates agreed. Deviations from $1/f^x$ were found with high theta peaks, which gave steeper slopes by regression, and high amplitude beta and gamma peaks that gave less steep slopes "(-1.0)" in D.

3.2. Simulation of ECoG PSD over a range of slopes.

Examples are shown in Fig. 3, A of the kernels from Equation (1) for decay rate α = 1/s with rise rate β = 1000/s and 10/s. Frames B – D show examples at the limits of the ranges of variation of α and β. The inflection frequency between the flat and steep segments varied from 1 to 3 Hz; values were uncertain owing to curvature in the range and to variation in the PSD with change in the seed for the random numbers. Conformance to the power-law distribution of the PSD (Fig. 6) held over the range of the rise time constant β = 3000/s to 10/s for frequencies above the inflection frequency. The slopes of the simulated PSD were determined by linear regression in the range of 10-100 Hz. The exponents of $1/f^x$ varied as a function of the rise rate β (Fig. 6) between 2 and 4 (negative of the slopes -2 to -4).

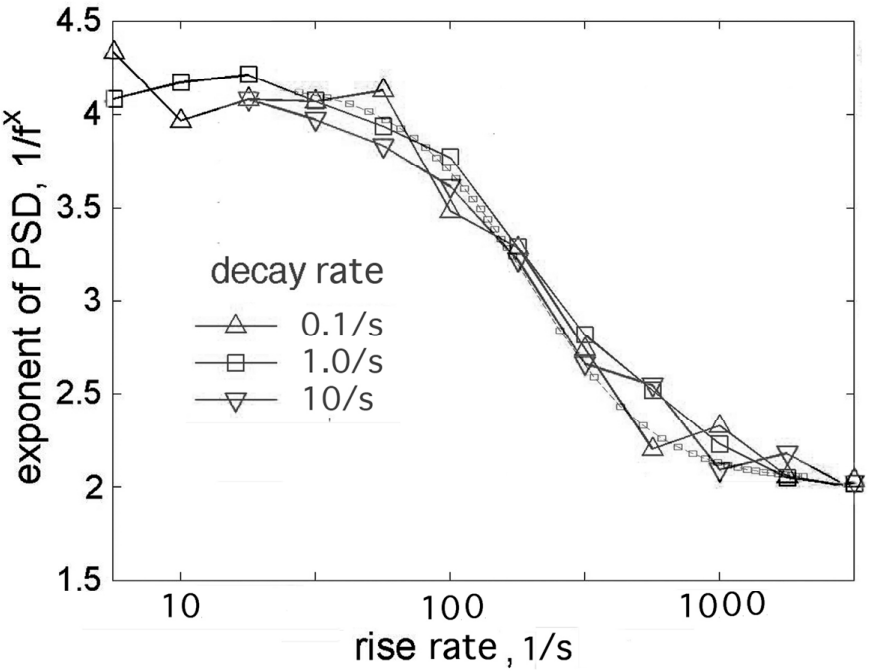

Fig. 6. The exponents x (negative of slope in $1/f^x$) depended on rise rate, β, not on decay rate, α. The data were fitted with equation (2) derived from the 2-pole filter.

$$x = 2 [2 - \alpha^2 / (\alpha^2 + 125^2) - \beta^2 (\beta^2 + 125^2)] \quad (2)$$

Variation in the decay rate, β, had no effect on the slope (Fig. 6). Instead it determined the roll-off frequency (Fig. 1, A-D and Fig. 5, B-D). The PSD were derived for the impulse responses in Fig. 2 by using the values of the decay rates in equation (1) for and β and α approximating the rise and decay rates with the values given in Fig. 2 and Fig. 7. The roll-off frequencies of the evoked responses approached or exceeded 10 Hz, which was well above the range observed in the PSD from ECoG. The observed roll-off frequencies indicated that the range of self-stabilized ECoG was well below the observable range of PSTH (Fig. 3, B).

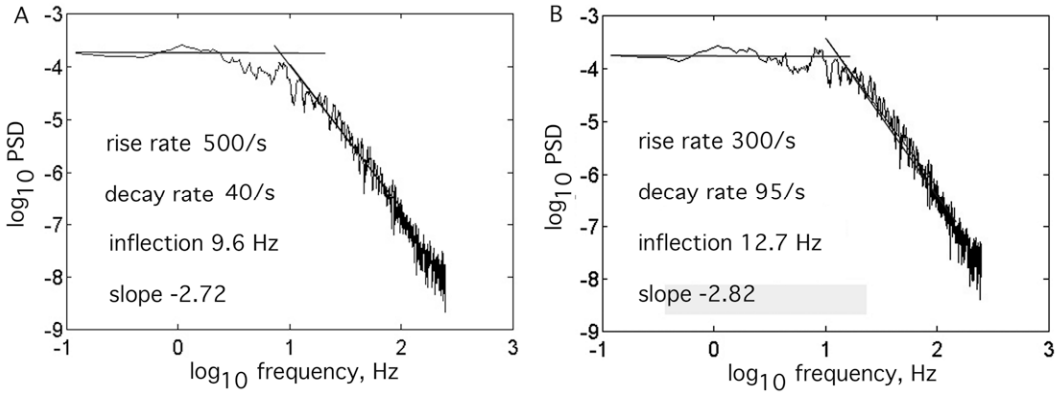

Fig. 7. The impulse responses in Fig. 5 are approximated by equation (1), with the decay rate and rise rate taken from Table 2 in Freeman [1974]. These kernels were convolved with the random pulse trains giving the simulated ECoG, from which the PSD were calculated by the multitaper method for the periodogram.

4. Discussion

Interpretation of this simulation is based on a model of the mechanism generating the background ECoG, which is seen in resting states, and which is characterized by the PSD conforming to the shape $1/f^x$. The proposed mechanism is based in mutual excitation among excitatory cells, which can be modeled as a positive feedback loop by dividing a population of excitatory neurons into transmitting and receiving neurons, with continuous renewal within the same population [Freeman, 1974]. The analysis was made possible by study of a neural population in the olfactory bulb, the periglomerular cells, for which the impulse response shows no evidence of inhibition; the neurons are GABAergic, but they have a high intracellular concentration of chloride ions [Siklós et al., 1995], so the effect on GABA A receptors is depolarizing. The mean rate constants for axosynaptic transmission and passive membrane decay provide the open loop parameters, and the interaction strengths combining synaptic weights and the sensitivity of trigger zones determine the positive feedback gain. A piece-wise linear model using ordinary differential equations gives the form of the impulse response to an electric stimulus as specified by a sum of exponential terms approximated by equation (1). The exponents are evaluated by fitting the impulse responses in the PSTH to evaluate the closed loop rate constants of the impulse responses.

The stability of the background at unity gain is governed by a non-zero point attractor, by which the level is homeostatically regulated. Under normal sensory bombardment the stable operating point is predicted to give finite values for α. The location of the inflection frequency in PSD of ECoG between 1 Hz and 10 Hz indicates typical values between 0.1/s and 10/s for prevailing steady state input levels. Yet the decay rates from the evoked activity ranged from 40/s to 95/s, which were far above the physiological range. Fig. 3, B then shows the degree to which the evoked activity deviates from normal, owing to the intensity of activation by electrical stimulation that is needed to observe the evoked activity by driving it far above the background level. This is verified by simulating the PSD of the evoked activity (Fig. 7), which show the inflection point as located above 9 Hz, outside the range for ECoG roll-off frequencies of the ECoG PSD.

It should now be clear that each pulse from an excitatory neuron at unity gain triggers a cascade of excitatory synaptic potentials, which sum in the cortical neuropil to give the ECoG. By extrapolation in Fig. 3 to very near threshold, the impulse response at rest has a very rapid rise and a very slow decay. The exponent, x, of the PSD in the 10-100 Hz range increases with decreasing rise rate, β, at all values of the decay rate, α. The impulse response shows a decrease in β and an increase in α with response amplitude (Fig. 1), which increases the roll-off frequency of the PSD with increasing amplitude of activity. The underlying cause is the decrease in positive excitatory feedback gain below unity, owing to the increase in the effect of the refractory periods with increased amplitude [Freeman, 1979]. With increasing stimulus intensity the crest of the impulse response is rounded (Fig. 5, A), which reflects the more sluggish response of the positive feedback system with reduced positive feedback gain. The rounding of the impulse response results in loss of high frequencies and an increase in the steepness of the PSD.

The increased steepness of slope in sleep compared with waking can be explained by postulating a sustained background excitatory input to cortex, together with reduction in the intrinsic background activity level, so that the refractory periods are more effective in limiting interactions. The exponent x can increase either with increased input at fixed background or decreased background at fixed input or both. The steeper slopes in slow-wave sleep reflect lower background rates of firing, whether from changes in refractory periods or neuromodulatory regulation or other aspects of sensitivity to input.

The detailed model [Freeman, 1975] shows that rise times are shaped by the sum of several exponential terms. These terms are important at the microscopic level. At the mesoscopic level of the ECoG the details are not significant, and the cumulative effects of the multiple sources of delay in neural transmission can be collapsed into a single term, β (Fig. 2), just as multiple factors in microscopic refractory periods can be incorporated into the single mesoscopic exponential term for β in equation (1).

Inhibition providing negative feedback does not play a direct role in stabilization of ECoG. It becomes important when subjects actively engage the environment by intentional action. Prominent oscillations appear in the ECoG from negative feedback, which are manifested in PSD peaks. The PSD does not then conform to a power-law distribution. Values of the slope from fitting a straight line with least squares criterion of goodness of fit in those cases are not valid, and random numbers are not appropriate for modeling such structured, nonrandom activity.

References

Abeles M [1991] Corticonics: Neural Circuits of the Cerebral Cortex. New York: Cambridge UP.

Barrie JM, Freeman WJ, Lenhart M [1996] Modulation by discriminative training of spatial patterns of gamma EEG amplitude and phase in neocortex of rabbits. J Neurophysiol 76: 520-539.

Elul R [1972] The genesis of the EEG. Int Rev Neurobiol 15: 227-272.

Freeman WJ [1974] A model for mutual excitation in a neuron population in olfactory bulb. Trans. IEEE Biomedical Engineering 21: 350-358.

Freeman WJ [1975] Mass Action in the Nervous System. New York: Academic Press. © 2004: http://sulcus.berkeley.edu/MANSWWW/MANSWWW.html

Freeman WJ [1979] Nonlinear gain mediating cortical stimulus-response relations. Biol Cybern 33:237-247.

Freeman W.J. [2004a] Origin, structure, and role of background EEG activity. Part 1. Analytic amplitude. Clin Neurophysiol 115: 2077-2088. http://repositories.cdlib.org/postprints/1006

Freeman W.J. [2004b] Origin, structure, and role of background EEG activity. Part 2. Analytic phase. Clin. Neurophysiol. 115: 2089-2107.

Freeman W.J. [2005] Origin, structure, and role of background EEG activity. Part 3. Neural frame classification. Clin. Neurophysiol. 116 (5): 1118-1129. http://authors.elsevier.com/sd/article/S1388245705000064

Freeman WJ [2006a] Origin, structure, and role of background EEG activity. Part 4. Neural frame simulation. Clin. Neurophysiol. 117: 572-589.

Freeman WJ [2006b] Definitions of state variables and state space for brain-computer interface. Part 1. Multiple hierarchical levels of brain function. Cognitive Neurodynamics 1(1): 13-14. http://dx.doi.org/10.1007/s11571-006-9001-x

Freeman WJ [2007] Definitions of state variables and state space for brain-computer interface. Part 2. Extraction and classification of feature vectors. Cognitive Neurodynamics 1(2): 85-96.

Freeman WJ, Holmes MD, West GA, Vanhatalo S [2006] Fine spatiotemporal structure of phase in human intracranial EEG. Clin. Neurophysiol. 117: 1228-1243.

Freeman WJ, Zhai J [2007] Deriving 1/f form of human EEG spectrum from summed random pulse trains. International Workshop on Nonlinear Brain Dynamics (IWNBD'07) 9-10 June 2007, Zhejiang University, Hangzhou, China.

Percival DB, Walden AT [1993] Spectral Analysis for Physical Applications: Multitaper and Conventional Univariate Techniques, Cambridge University Press.

Raichle ME [2006] The brain's dark energy. Science 314: 1249-1250.

Schroeder M [1991]. Fractals, Chaos, Power Laws. Minutes from an Infinite Paradise. San Francisco: WH Freeman.

Siklós L, Rickmann M, Joó F, Freeman WJ, Wolff JR [1995] Chloride is preferentially accumulated in a subpopulation of dendrites and periglomerular cells of the main olfactory bulb in adult rats. Neuroscience 64: 165-172.